Diamond & Related Materials 29 (2012) 13–17

Contents lists available at SciVerse ScienceDirect

Diamond & Related Materials

journal homepage: www.elsevier.com/locate/diamond

Charge dissipation layer optimisation for nano-scale electron-beam lithography pattern definition onto diamond

A.I.M. Greer *, D.A.J. Moran

School of Engineering, Rankine Building, University of Glasgow, Glasgow, G12 8QQ, United Kingdom

ARTICLE INFO

Article history:
Received 9 February 2012
Received in revised form 2 July 2012
Accepted 5 July 2012
Available online 14 July 2012

Keywords:
Diamond
Discharge
Nano
Electron-beam lithography
Aluminium

ABSTRACT

This paper demonstrates that the pattern feature size achieved for electron beam lithography (EBL) on diamond substrates can be minimised through optimisation of the thickness of a surface deposited metallic discharge layer. The purpose and benefits of a charge dissipation layer are presented and the subsequent trade-off with feature size examined. 5 nm of Al is demonstrated to be the optimum thickness of charge dissipation layer for polymethyl methacrylate (PMMA) resist on polycrystalline diamond as the feature size retains a similar variance to thicker layers, has good reproducibility and ultimately produces the smallest feature sizes. PMMA can be used as either a metal deposition mask, or an etch mask for SiO_2 which in turn can be used as an etch mask for diamond. Using this process we have demonstrated pattern transfer and metallisation of features onto diamond and SiO_2 coated diamond down to a dimension of 20 nm.

1. Introduction

Diamond is a material which is finding an ever growing variety of applications within nano-technology for applications such as nano-imprint lithography [1], biological implant coatings and interfaces [2], particle sensing [3] and electronics [4]. Electron-beam lithography (EBL) is an essential step in producing the required feature size for many of these applications. In its intrinsic form, diamond is essentially an insulator due to its large band-gap of 5.45 eV [5], so is unable to effectively dissipate introduced charge. During EBL utilising diamond substrates, charge may build up on the surface, leading to deflection of the electron beam (e-beam), causing the pattern written in the resist to differ from the design [6]. A common method of alleviating this problem is to deposit a layer of electrically conductive material known as a charge dissipation layer (CDL) on top of the electron-sensitive resist [7], shallow enough for electrons to penetrate and pattern the resist below but thick enough to easily dissipate charge. Due to radial beam divergence, focusing an electron-beam on the surface of a sample with a CDL results in the thickness and composition of the CDL distorting the effective spot size experienced by the resist and modifying the desired pattern feature size and shape [8]. Little evidence has been reported on the impact of this process on ultra-nano feature pattern potential on diamond. The objective of this work was to determine the optimum thickness of CDL for ultra-nano pattern transfer using polymethyl methacrylate (PMMA) resist masks on polycrystalline diamond.

Pattern transfer onto a substrate by EBL is typically performed by one of two processes following resist development; etching, whereby the resist acts as a mask to protect the substrate surface from an etch chemistry [9], and deposition and lift-off of material onto the surface of the substrate [10]. Metals are deposited in this manor for a range of applications on diamond and can also be used as a mask [11] or catalyst [12] for etching. PMMA is readily attacked by traditional diamond dry etch recipes [13], so is not typically used as a dry etch mask itself. For this work PMMA is instead utilised as a deposition and lift-off mask for metal features onto the diamond surface. In this instance the metal features act purely as an indicator of the dimensions and shape of the resist profile at the interface with the diamond substrate, allowing for inspection of potential distortion of or deviation from the designed pattern. In addition to pattern transfer via etching, the ability to produce nano-scale metallic contacts onto diamond is vital for devices such as high frequency field effect transistors [14] and quantum probes [15].

2. Material and method

A 580 μm thick, 10 mm × 10 mm, polycrystalline diamond substrate with ~50 μm grain size sourced from Element Six was used as the substrate material for this series of experiments. The sample was initially subjected to acid (HF) and solvent cleaning. Thereafter the roughness was confirmed to be 0.5 nm Ra with an atomic force microscope (AFM). PMMA was then spin-coated on top of the sample as a bi-layer with undercut to aid lift-off of deposited material onto the diamond surface.

Al is often used as a CDL for electron-beam patterning of insulating substrates because of its good electrical conductivity, its relative low

* Corresponding author.
E-mail address: a.greer.1@research.gla.ac.uk (A.I.M. Greer).

0925-9635/$ – see front matter © 2012 Elsevier B.V. All rights reserved.
doi:10.1016/j.diamond.2012.07.003

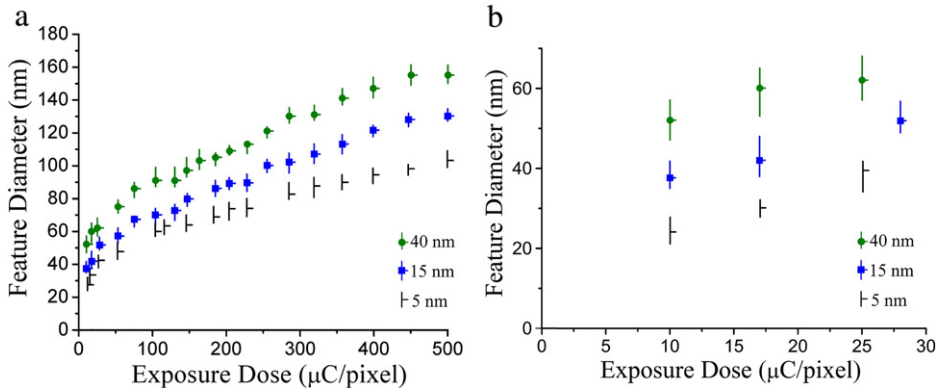

Fig. 1. (a) A comparison plot of feature diameter (nm) against dose (μC/pixel) for three samples containing an Al CDL on PMMA on diamond. The bottom contour is the 5 nm thick version, the middle one 15 nm and the top contour 40 nm. (b) An expansion of the first 30 μC/pixel results. The vertical lines for all plots represent error bars covering 8 measurements per inspected dose.

cost and its availability in many fabrication facilities. Previous work has reported the use of a 40 nm thick Al layer for the purpose of a CDL [16]. Therefore 40 nm of Al was adopted as an initial thickness for experimentation. This was then reduced to investigate the resulting impact on EBL defined pattern feature size and shape, and the point at which the Al layer ceases to operate efficiently as a CDL. This data was also compared with a control run utilising a sample without any CDL. The Al was deposited on top of the PMMA using an electron-beam metal evaporator.

Pattern transfer into the PMMA/Al stack was achieved using a Vistec Gaussian Vector Beam 6 (VB6) EBL tool with 12 nm beam spot size and operating at 100 kV accelerating voltage. The pattern design consisted of a square matrix of size 150 μm of single point exposures at 305 nm pitch. Since features were created with single point exposures, proximity effects were not a concern. The design was repeated on the sample for a range of doses from 10 to 500 μC/pixel. Doses below 10 μC/pixel were not examined as this level approached the underexposure region and feature sizes were reaching a scale where the processing environment needs to be kept meticulously consistent for accurate statistical comparison. Pixels were square with length 305 nm. After patterning the resist, the Al CDL was removed with Tetramethylammonium hydroxide. The PMMA was then developed in MIBK:IPA solution. Following development, an oxygen barrel asher was used to remove ~10 nm of residual PMMA. It was important to ensure that the developed patterns in the PMMA penetrated all the way through the resist to the surface of the substrate. In order to confirm the shape and depth of the exposed features at the PMMA/substrate interface, 60 nm of gold was evaporated using a metal evaporator. The gold coated PMMA was then lifted-off with acetone, leaving 60 nm high Au features. The gold features were then inspected using a Scanning Electron Microscope (SEM). To resolve the resultant metalized features and minimise charging of the diamond substrate within the SEM, a 5 nm layer of Au was evaporated over the sample surface. Analyses of the features involved capturing images for a range of doses across the sample after each run and processing them with IMAGEJ software [16]. For each dose, multiple sites were examined and the circularity and diameter of the point exposures measured. The feature diameter was recorded on a maximum, minimum, average graph against exposure dose (Fig. 1). The average diameter was calculated using Eq. (1) (used to calculate average feature size, where '*n*' is the total number of sites, '*i*' refers to a site and '*a*' is the value of a site).

$$Ave = \frac{1}{n}\sum_{i=1}^{n}(a_i) \tag{1}$$

An alternative approach for nano-patterning diamond with PMMA is to first use the PMMA as an etch mask to transfer a pattern into a SiO_2 coating deposited on the diamond surface, which then itself acts as a mask for reactive ion etching [17]. Unlike metal mask layers, SiO_2 is not a good electrical conductor; diamond with a SiO_2 coating also requires the incorporation of a CDL during EBL. To investigate the impact of the presence of such a dielectric layer between the diamond and electron sensitive resist, the experiment was repeated with ~120 nm of chemical vapour deposited SiO_2 beneath the PMMA.

3. Results and discussion

3.1. Effect of Al CDL thickness on PMMA above diamond

As an initial reference point, 40 nm of Al proved to be an effective CDL with average feature size plotted against dose following a clear contour. The maximum variance in feature size was no greater than 13 nm for all inspected sites. This data is presented in Fig. 1. In addition, the feature geometry remained circular across the range of doses tested. At the lowest dose examined (10 μC/pixel) the average feature size was 52 nm (minimum size = 47 nm), and at the largest dose (500 μC/pixel) the average feature size was 155 nm.

The CDL thickness was then decreased to 15 nm and the resultant feature dimensions compared with the 40 nm Al CDL results. It can be seen from Fig. 1 and Table 1 that the feature sizes obtained by reducing the CDL thickness are smaller for all tested doses. The smallest features had an average diameter of 38 nm, compared to 52 nm for the thicker CDL. The maximum deviation was also smaller at 12 nm and the feature shape maintained good circularity across the range of doses tested.

The CDL was then thinned down from 15 nm to 5 nm and again the resultant features were inspected at varied exposure dose sites. The results followed a steady contour and was similar to that of the 15 nm layer; however a shallower gradient for the average feature size versus exposure dose slope was observed. For exposures below 20 μC/pixel the features begin to lose true circularity because even small defects around the perimeter become more relative as the feature size approaches 20 nm. Although the reproducibility of the exact

Table 1
Summary of key feature size statistics for the three effective CDL thicknesses tested (40 nm, 15 nm and 5 nm) on diamond.

CDL thickness	Average feature size at 500 μC/pixel	Average feature size at 10 μC/pixel	Minimum feature size at 10 μC/pixel	Maximum deviation of feature size at any dose
40 nm	155 nm	52 nm	47 nm	13 nm
15 nm	130 nm	38 nm	35 nm	12 nm
5 nm	103 nm	24 nm	21 nm	12 nm

CDL = charge dissipation layer, PMMA = polymethyl methacrylate, IPA = isopropyl alcohol, EBL = electron-beam lithography, MIBK = methyl isobutyl ketone, HF = hydrofluoric.

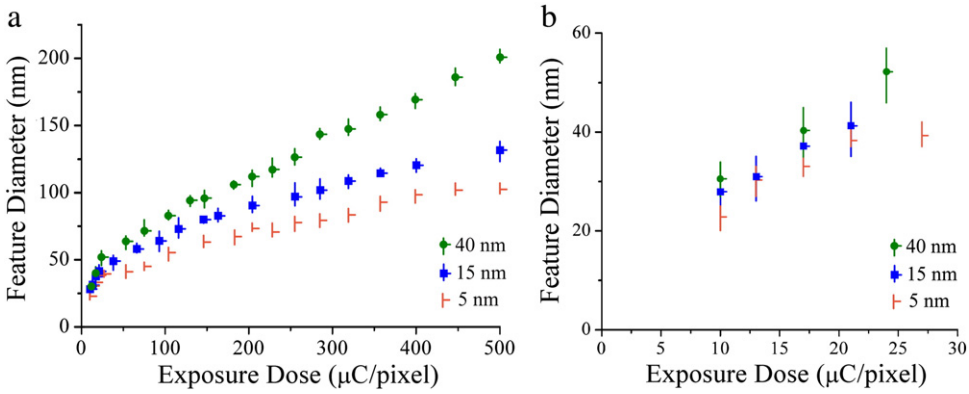

Fig. 2. (a): A comparison plot of feature diameter (nm) against dose (μC/pixel) for three samples containing an Al CDL on PMMA on top of the diamond coated with 120 nm SiO_2. The bottom contour is the 5 nm thick version, the middle one 15 nm and the top contour 40 nm. (b): An expansion of the first 30 μC/pixel results. The vertical lines for all plots represent error bars covering 8 measurements per inspected dose.

feature shape at sub-20 μC/pixel is difficult to modulate, the features do retain a controllable size with maximum deviation again measured to be 12 nm. The features with the smallest dimensions were observed at the lowest implemented dose of 10 μC/pixel. These had a diameter of 24 nm. In comparison with the smallest features achieved with the 40 nm CDL (47 nm diameter), this corresponds to a reduction of 49% in minimum achievable feature size through minimisation of the CDL thickness. The key statistical findings from this trial and the previous two experiments are summarised in Table 1.

A control run with no CDL and a sample with a 2 nm Al CDL were also similarly patterned and inspected. In both cases metal features, including larger marker structures, were completely removed during the lift-off process. It is assumed that due to the lack of CDL on the control and the consumption of Al to native oxide on the 2 nm version, the build up of surface charge leads to deformation of the resist profile and poor lift-off yield.

3.2. Effect of Al CDL thickness on PMMA above SiO_2 coated diamond

The alternative method of utilising PMMA for pattern transfer to diamond is to use it as an etch mask for pattern transfer first into a material better suited to withstand typical diamond RIE chemistry. SiO_2 is a typical material used for this process [17], and so positive photo resist such as PMMA is often used as a mask to initially pattern a SiO_2 layer on the diamond surface [18]. In order to determine whether a SiO_2 layer has any impact on the results demonstrated without a surface dielectric layer, the experiment was repeated with 120 nm of SiO_2 between the PMMA and the diamond.

All of the metal thicknesses tested in Section 3.1 were retested as part of the stack including the SiO_2 layer. 40 nm of Al again proved to be effective and sufficient as a CDL producing circular features across the range of tested exposure doses. In this instance when the average feature size was plotted against dose, it too followed a clear contour however it is moderately different from the 40 nm layer tested without SiO_2. In this instance the contour is more linear and covers a wider range of feature sizes with extensions at both ends of the spectrum, as shown in Fig. 2 (a). At the top end the average feature size was 201 nm (30% greater than the equivalent with no SiO_2 layer) and at the lowest dose the features were on average 30 nm diameter (a reduction of over 40%). The sample did however share the same variance of 13 nm with the SiO_2-free version.

The 15 nm thick Al CDL faired more analogous to the non-coated diamond version for the top half of the exposure spectrum considered. As the dose decreased toward the 10 μC/pixel mark the gradient becomes less steep and deviates from the SiO_2-free counterpart. The maximum site variance remained at a similar value of 11 nm. The feature shape maintained good circularity across the range of doses tested and the average feature diameter at the lowest tested dose was 23 nm.

The difference between the SiO_2 coated and non-coated samples was least noticeable for the 5 nm version of CDL. At both the maximum and minimum tested doses there was only a difference of 1 nm in average feature size. The site variance was also recorded to be within 1 nm of the SiO_2-free version. The feature circularity was good across the dose range but like the non-coated diamond sub-20 μC/pixel impinged on the limits of accurate and reproducible shape for the lift-off of metal features. At the lowest tested dose the average feature size recorded was the smallest achieved in these experiments at 23 nm. The smallest features measured for individual exposure sites were 20 nm in diameter (as shown in Fig. 3).

The effect of reducing the CDL thickness has been shown to decrease the obtainable feature size in all cases. The biggest impact was found to be present on the SiO_2 coated sample between the 40 nm CDL and 5 nm CDL at the 500 μC/pixel site. At this site, the effect of using a 40 nm thick CDL instead of a 5 nm thick CDL corresponds to a 100% increase in obtainable feature size. The key statistical findings from the SiO_2 coated trials are summarised in Table 2.

Similar to the experiments excluding a SiO_2 layer, the impact of further reducing the CDL thickness from 5 nm to 2 nm of Al was then tested. In contrast to the results without SiO_2 present whereby metallisation was unsuccessful, metallised features were observed across the sample. In general, the inspected features were larger than those achieved using the 5 nm CDL. In addition many were found to be more elliptical than circular and became much defined

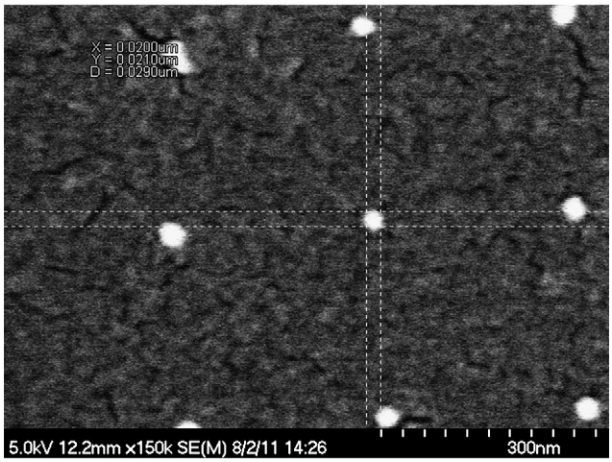

Fig. 3. SEM image of a 20 nm diameter circular Au feature on SiO_2 coated diamond after patterning with a 5 nm CDL.

Table 2
Summary of key feature size statistics for the three effective CDL thicknesses tested (40 nm, 15 nm and 5 nm) on SiO_2 coated diamond.

CDL Thickness	Average feature size at 500 μC/pixel	Average feature size at 10 μC/pixel	Minimum feature size at 10 μC/pixel	Maximum deviation of feature size at any dose
40 nm	201 nm	30.5 nm	27 nm	13 nm
15 nm	132 nm	28 nm	24 nm	11 nm
5 nm	102 nm	23 nm	20 nm	11 nm

rod shapes at doses of 59 μC/pixel and below (as can be seen in Fig. 4). No features were present for doses below 24 μC/pixel utilising a 2 nm thick CDL.

Finally, a control run with no CDL was repeated for the diamond with the SiO_2 coating. The average feature size between the doses of 100 μC/pixel and 500 μC/pixel follows a similar gradient to the sample patterned with 15 nm of Al. However, below 100 μC/pixel the feature size plateaus at ~65 nm, indicating a threshold for the minimum feature size obtainable without a CDL. The features also exhibited a change in shape at the lower end of the exposure spectrum. The features change from round spots to elongated lines as the dose drops below 42 μC/pixel. There were no features detected below 17 μC/pixel which suggests that this dose range is insufficient for pattern transfer into this resist structure on polycrystalline diamond without a CDL. The maximum deviation for each dose was also far less consistent than any of the samples patterned with a CDL thicker than or equal to 5 nm. The feature shape change, increase in size and higher value of suitable dose for pattern transfer were properties that the CDL-free control sample shared with the 2 nm CDL. Given the exposure of the 2 nm Al layer to ambient conditions following deposition, it is proposed that native oxidation of this layer destroys its conductive properties, rendering it ineffective as a charge dissipation layer. Both the control and 2 nm CDL sample therefore suffer from undesirable charging of the diamond surface during EBL. The explanation for the variation in yield of metallised features between samples with reduced CDL thickness (i.e. 2 nm CDL and no CDL) on non-coated and those on SiO_2 coated diamond is yet unclear but is perhaps related to the charging effects and potential divergence of the electron beam in the presence of the SiO_2 dielectric layer.

Evidence for the process by which charging effects can impact on e-beam sensitive resist feature size and dimension is discussed by Kudryashov et al. [6]. In their paper it is stated that low secondary emission coefficients and non-conductive substrates result in large amounts of exposure charge being trapped in an e-beam resist on the surface of the sample. It can be noted that diamond is a non-conductive substrate with a low secondary emission coefficient. Hence, according to the conditions discussed by Kudryashov et al., the samples analysed in this work are susceptible to charge trapping and feature deformity if the CDL is not thick enough to operate effectively. Both the SiO_2 coated and non-coated diamond samples experienced feature deformity for sub-5 nm CDL patterning and are likely related to charge trapping as a consequence of not having a thick enough CDL to effectively dissipate excess charge.

The convergence observed in Fig. 2 between the 5, 15 and 40 nm CDL feature size plots is most likely related to the lower concentration of incident electrons per unit area at lower dose leading to a lower build up of surface charge and associated e-beam deflection. Hypothetically, a dose corresponding to one electron would produce the same size of feature in resist regardless of CDL thickness. The plots for the SiO_2-free samples also exhibit decreased deviation (although remain more discrete) at the lower end of the dose spectrum and this is also attributed to the same effect.

4. Conclusion

A range of Al charge dissipation layer (CDL) thicknesses has been investigated for electron-beam patterning of polycrystalline diamond substrates. These results demonstrate that with no or very thin CDL, minimum feature size, shape and reproducibility are limited by surface charging. CDLs with thicknesses of 5 nm and above worked effectively but radial beam divergence results in an increase in minimum feature size as the CDL thickness increases. These results were also proven to be applicable with a 120 nm SiO_2 layer present between the resist and the diamond surface. The smallest features

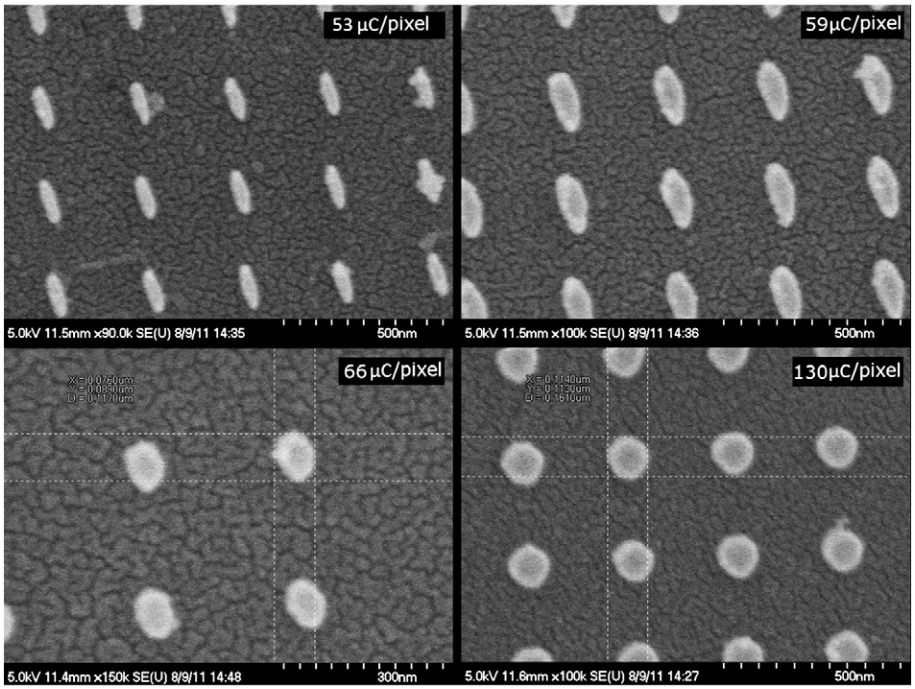

Fig. 4. SEM images of Au features deposited onto polycrystalline diamond after EBL patterning using a 2 nm Al CDL. Top left: 53 μC/pixel exposure resulting in rod shaped features, top right: 59 μC/pixel exposure resulting in elongated oval shaped features, bottom left: 66 μC/pixel exposure resulting in slightly oblong ellipse shaped features, bottom right: 130 μC/pixel exposure where features exhibited improved circularity.

achieved in this work include metalized dots of 20 nm (diameter) and were obtained using a 5 nm thick Al CDL on a SiO_2 coated diamond substrate. We conclude that 5 nm is the optimum CDL thickness for nano-scale patterning of diamond substrates by electron beam lithography, providing minimal pattern distortion, good reproducibility and ultimately the smallest feature size.

Acknowledgements

This work was funded by the EPSRC and all processing was carried out in the James Watt Nanofabrication Centre (JWNC) at The University of Glasgow. We are grateful for the support and training provided by the JWNC technical staff.

References

[1] K. Lister, S. Thoms, D. Macintyre, C. Wilkinson, J. Weaver, B. Casey, J. Vac. Sci. Technol., B: Microelectron. Nanometer Struct. 22 (2004) 3257.
[2] X. Xiao, J. Wang, C. Liu, J.A. Carlisle, B. Mech, R. Greenberg, D. Guven, R. Freda, M.S. Humayun, J. Weiland, O. Auciello, J. Biomed. Mater. Res., B: Appl. Biomater. 77B (2006) 273–281.
[3] C.E. Nebel, B. Rezek, D. Shin, H. Uetsuka, N. Yang, J. Phys. D: Appl. Phys. 40 (2007) 6443.
[4] D. Moran, D. MacLaren, S. Porro, H. McLelland, P. John, J. Wilson, Microelectron. Eng. 88 (2011) 2691–2693.
[5] M.N. Yoder, IEEE Trans. Electron Devices 43 (1996) 1633–1636.
[6] V.A. Kudryashov, V.V. Krasnov, P.D. Prewett, T.J. Hall, Microelectron. Eng. 35 (1997) 165–168.
[7] W. Zhang, A. Potts, D.M. Bagnall, B.R. Davidson, Thin Solid Films 515 (2007) 3714–3717.
[8] L.D. Dickson, Appl. Opt. 9 (1970) 1854–1861.
[9] A.I.M. Greer, K. Seunarine, A.Z. Khokhar, X. Li, D.A.J. Moran, N. Gadegaard, Phys. Status Solidi A 1–5 (2012), http://dx.doi.org/10.1002/pssa.201200057.
[10] J. Taniguchi, Y. Tokano, I. Miyamoto, M. Komuro, H. Hiroshima, Nanotechnology 13 (2002) 592.
[11] D. Tran, C. Fansler, T. Grotjohn, D. Reinhard, J. Asmussen, Diamond Relat. Mater. 19 (2010) 778–782.
[12] W. Smirnov, J. Hees, D. Brink, W. Müller-Sebert, A. Kriele, O. Williams, C. Nebel, Appl. Phys. Lett. 97 (2010) 073117.
[13] F.D. Egitto, Pure Appl. Chem. 62 (1990) 1699–1708.
[14] M.J. Dalby, N. Gadegaard, R. Tare, A. Andar, M.O. Riehle, P. Herzyk, C.D.W. Wilkinson, R.O.C. Oreffo, Nat. Mater. 6 (2007) 997–1003.
[15] A.W. Schell, G. Kewes, T. Hanke, A. Leitenstorfer, R. Bratschitsch, O. Benson, T. Aichele, Arxiv preprint, arXiv:1103.2019 2011.
[16] R. Dylewicz, S. Lis, R. De La Rue, F. Rahman, J. Vac. Sci. Technol., B: Microelectron. Nanometer Struct. 28 (2010) 817.
[17] S. Okuyama, S.I. Matsushita, A. Fujishima, Langmuir 18 (2002) 8282–8287.
[18] O. Makarova, R. Divan, N. Moldovan, D. Rosenmann, C.M. Tang, J. Vac. Sci. Technol., B: Microelectron. Nanometer Struct. 28 (2010) C6P42–C46P47.